Journal of the European Ceramic Society 7 (1991) 335–341

A Description of Microstructure Applied to the Thermal Conductivity of AlN Substrate Materials

S. Ruckmich, A. Kranzmann, E. Bischoff & R. J. Brook

Max-Planck-Institut für Metallforschung, Heisenbergstrasse 5, 7000 Stuttgart 80, Germany

(Received 17 September 1990; revised version received 20 December 1990; accepted 7 January 1991)

Abstract

Pressureless sintered polycrystalline AlN substrate materials doped with CaO were annealed in a non-oxidizing atmosphere. During the annealing, the geometrical microstructure of the AlN polycrystal changed, resulting in the production of progressively more planar grain boundaries. A description of microstructure was developed to describe the observed microstructural variations in AlN during annealing. The minimizing of the grain boundary length per unit area of sample cross-section was coupled with an increase in the thermal conductivity and with a slight decrease in strength which could not be fully explained by the effects of grain growth. During annealing, line defects occurred in a fraction of the grains; these were ordered in defect bands and were sites for precipitation of the sinter additive. Changes in geometric structure cannot alone explain increases in conductivity up to 219 $W m^{-1} K^{-1}$. Such high thermal conductivities are always associated with pure AlN crystals.

Drucklos mit CaO-Zusätzen gesinterte AlN-Substratkeramiken wurden in reduzierender Atmosphäre ausgelagert. Während der Glühung änderte sich die Form der AlN-Körner von mehr sphärischer zu mehr polygoner Gestalt. Dies ist gleichbedeutend mit ebeneren Korngrenzen. Ein einfacher Parameter wurde entwickelt, welcher in der Lage ist, diesen Vorgang zu beschreiben. Die Verkleinerung der linearen Korngrenzenlänge pro Einheitsfläche in der betrachteten Schliffebene führt zu einem Anstieg der Wärmeleitfähigkeit und einer geringen Festigkeitsabnahme. Die verbesserte Wärmeleitfähigkeit ist nicht durch das vergrößerte Korn allein erklärbar. Neben den Änderungen der geometrischen Gefügestruktur wurde die Bildung von Liniendefekten beobachtet, die in Bändern angeordnet vorlagen und gemeinsam mit Ausscheidungen von sinteradditivhaltiger Phase auftraten. Der beobachtete Anstieg der Wärmeleitfähigkeit auf 219 $W m^{-1} K^{-1}$ kann nicht allein durch Änderungen der geometrischen Gefügeparameter erklärt werden. Solch hohe Wärmeleitfähigkeiten sind immer an ein chemisch reines AlN-Korn gebunden.

On a recuit, sous atmosphère non oxydante, des substrats polycristallins d'AlN dopé au CaO et consolidés par frittage naturel. La géométrie de la microstructure de l'AlN polycristallin évolue au cours du recuit, conduisant progressivement à des joints de grains de plus grande planéité. On a développé une description de la microstructure permettant de rendre compte des variations de microstructure de l'AlN lors du recuit. La minimisation de la longueur de joint de grain par unité de surface de section droite de l'échantillon était associée à une élévation de la conductivité thermique et à une légère décroissance de la résistance mécanique qui ne peut pas être entièrement expliquée par des effets de croissance de grains. Lors du recuit, des défauts en ligne sont apparus dans certains grains; ils étaient ordonnés en bandes de défauts et constituaient des sites de précipitation des additifs de frittage. Les changements de structure géométrique ne peuvent, à eux seuls, expliquer les augmentations de la conductivité, cette dernière pouvant atteindre jusqu'à 219 $W m^{-1} K^{-1}$. Des valeurs de conductivité thermique aussi élevées sont toujours associées à des cristaux d'AlN pur.

1 Introduction

In recent years, AlN has been much investigated with the aim of influencing the thermal conductivity by special choice of sinter additives. It has been proposed that the sinter additive can bond the oxygen impurity; it should be crystallized after sintering because crystalline phases would limit any decrease in the thermal conductivity.[1,2] The most common sinter additives are the rare earths and

Journal of the European Ceramic Society 0955-2219/91/$3.50

CaO, although certain fluorides such as YF_3 have also been recently investigated. All these dopants act to densify the material by liquid-phase sintering, using the liquid phase formed between Al_2O_3, the additive and dissolved AlN. The goal of the present investigation has been to describe the microstructural development, the changes in the heat conductivity and the mechanical character of AlN materials as a consequence of annealing at temperatures comparable to the ordinary sintering temperature. AlN doped with CaO has been investigated because it is easy to densify[3] and because the thermal conductivity is relatively high (about $100\,W\,m^{-1}\,K^{-1}$).

2 Microstructural Description

Thermal conductivity is sensitive to the form and volume fraction of the phases forming a material;[4] this is best discussed under the limiting assumption that the homogeneous volumes of one phase can be described as ellipsoids.[5] As predicted, the flattening of the AlN–AlN grain contacts and the elimination of the oxide phases should cause simultaneously an increase in the thermal conductivity, whereas the grain growth should decrease the mechanical strength. A combination of the topological parameter, as observable in a plane section, as mostly used by material scientists to describe microstructures, corners per grain and the fractal dimension can be readily used to describe the microstructural changes, as schematically shown in Fig. 1. In a plane section, the number of neighbours, N_N, at the beginning of microstructural development is not necessarily equal to the number of corners, N_C, of the forming polygonal outline of the grains. It is necessary for the making of topological statements to define a corner: a point on the boundary is a corner C if $R_l < 20\,D_G$, where R_l is the local radius and D_G the grain diameter. This definition is very similar to an alternative, which would use a special limit of the quotient between the length of a curve and the corresponding arc, the usual way to observe the curvature. The observation corresponding to this definition has the benefit of allowing the use of a hole stencil with holes of different radii to conclude whether a given point is or is not a corner. In this technique, the corners are easily counted. In a planar observation, the quotient between the mean number of corners per grain and the mean number of neighbours per grain is 1 if all grain outlines are polygons and zero if all grains are ball-like.

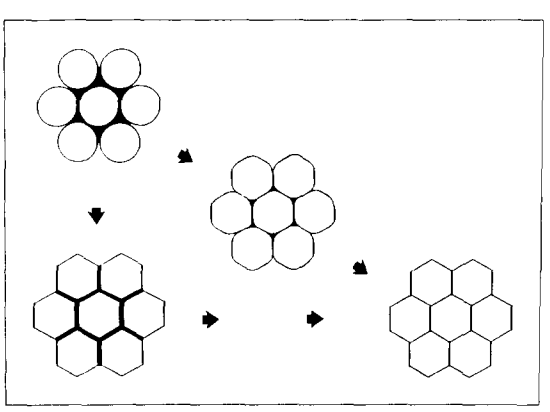

Fig. 1. Scheme of different microstructures with increasing thermal conductivity in the direction of the arrows. All grains are similar in shape parameters based on the length of the grain outline divided by grain area, or ratio of long and short axes.

In real observations, the connection lines between two edges are generally not perfectly linear. One parameter which reflects the size and form distribution is the fractal dimension. In analogy with the work of Richardson,[6] in which different coast lines are characterized by their fractal dimension, D_f, planar grain boundary networks can also be more fully described. An exact planar network with unit cell dimensions would show the fractal dimension, $D_f = 1$, which is equal to the topological dimension, D_t. An excellent treatise on the meaning of the mathematical dimension is published by Mandelbrot.[7]

With this information, the planarity, P_l, is defined as

$$P_l = \frac{N_C \cdot N_N^{-1}}{D_f \cdot D_t^{-1}} = \frac{N_C \cdot D_t}{N_N \cdot D_f} \qquad (1)$$

where $D_t = 1$, the topological dimension of a linear figure such as a boundary line on a surface. The parameter, P_l, varies between 0 and 1 and is easy to interpret. If, for example, there is a small amount of a second phase concentrated only in the triple points on the prepared surface, then the number of edges and the number of next neighbours will be equal and the numerator will be 1; however, the fractal dimension will be bigger than 1 and this will modulate the observed value to a lower planarity. If the microstructure can be observed in three dimensions, perhaps by scanning acoustic microscopy, then the fractal dimension of the three-dimensional array of the grain boundaries can be observed; normalization to the corresponding topological dimension, D_t, in eqn (1) will then be important.

If the second phase wets the grains, this kind of contact will be describable by modulations of P_l with the kind of contact. The probability of a direct contact AlN–AlN, C_{AA}, is nearly 1 if the grains are not wetted, is one if the second phase is evaporated, and is zero if all grains are wetted.[8]

3 Experimental Procedure and Results

3.1 Sample preparation

AlN powder (H. C. Starck, Berlin) and commercial CaO powder (Alfa, Karlsruhe) were mixed by attrition milling. For this process, quantities of 0·1 kg powder, 98·6 mass% AlN and 1·4 mass% CaO, together with 0·2 litre isopropanol and 0·75 kg Al_2O_3 milling balls were placed in a 500 ml porcelain container and moved by a steel stirrer.

The chemical quality of the powders is described in Table 1. A 0·7 mass% weight loss was produced by the evaporation of water during the decomposition of $Ca(OH)_2$ at $T \approx 400°C$ and a 0·2 mass% weight loss resulted from the thermal decomposition of $CaCO_3$ at $T \approx 700°C$ when the CaO was heated up to 1200°C in a thermogravimetric test. The water contamination in the form of $Ca(OH)_2$ can be neglected. During the milling process, the oxygen content of the AlN increased to 2·5 mass%.[3] This oxygen resulted at the surface of the AlN grains in the form of a hydroxide layer and reacted during sintering with the dopant materials.

The sintering process was conducted in a graphite-heated high-temperature furnace. A heating rate of 15°C min^{-1} was used to bring the samples to the sintering temperature of 1820°C. This temperature profile was developed prior to the start of this work.[3] All samples reached densities between 98·1 and 99·4% of the theoretical density. The weight loss of the samples was less than 1 mass%.

In contrast to the densification programme, the samples were heated up to the annealing temperature, $T_A = 1820°C$, at a rate of 80°C min^{-1}. Two different environments were chosen for the treatments. The first series of samples was heated in a BN container in the normal sintering environment; the second series was heated in a powder bed comprising 50 vol.% carbon black with a BET surface area of more than 100 $m^2 g^{-1}$ and 50 vol.% AlN powder. The reason for this change was the need of a reactive environment which could protect the samples against the influence of impurities arising from the furnace isolation and promote reactions involving the oxides vaporizing from the samples. After annealing for different times up to 44 h, the samples were polished and etched to allow investigations of the microstructure.

Table 1. Quality of the used raw powders

	Powder		
	AlN (quality A)	*CaO*	*AlN/CaO (milled powder)*
Supplier	H. C. Starck, Berlin	Alfa, Karlsruhe-	
Chemical analysis, mass%	Al: >65 N: 33 C: 0·05 O: 1·2 Fe: 0·01 Other: <0·1	Purity = 99·95%	Ca: 1 Si: 0·16

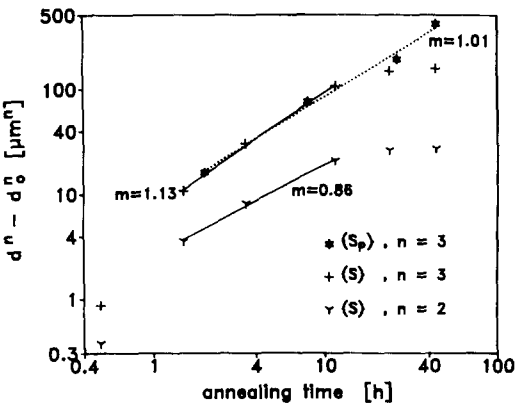

Fig. 2. Description of the grain growth by a power law shows that the grain growth of the grains is influenced by the atmospheric conditions.

3.2 Grain growth

During the first ten hours of annealing there is a difference in grain growth between samples annealed in the powder bed $\{S_P\}$ and those processed without the powder bed $\{S\}$. The grain growth of the powder bed samples can be exactly described by a power law of the form

$$\Delta D = d^n - d_0^n = \text{constant}\, t \qquad (2)$$

where t is the time, d the instantaneous grain diameter, d_0 the original grain diameter and where n has the value 3. Without the protective powder bed, $\log(\Delta D)$ versus $\log(t)$ gives a non-integer gradient between 2 and 3 in eqn (2) (see Fig. 2).

Without a powder bed, the second phase formed

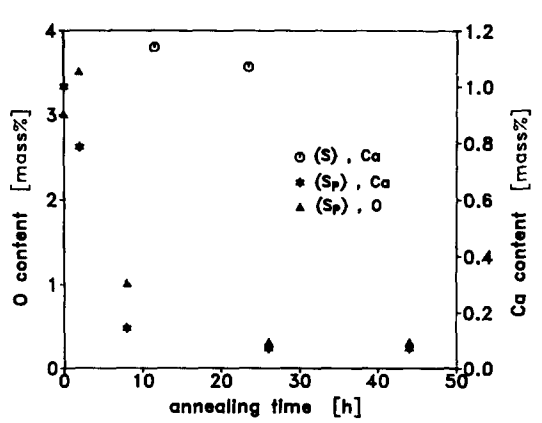

Fig. 3. Change of the Ca and O content during annealing of the sample sets $\{S_P\}$ and $\{S\}$.

from Ca, Al and O could not be eliminated; in contrast, the samples $\{S_P\}$ could be produced with Ca contents below 0·1 mass% after 20 h annealing time (see Fig. 3). X-Ray and TEM-EDX analysis demonstrated that the second phase changed in composition from $CaAl_4O_7$ to $CaAl_2O_4$ during tempering. The samples $\{S_P\}$ lost their triple point phase (Fig. 4), whereas the samples $\{S\}$ exhibited a residual grain boundary phase (Fig. 5).

3.3 Microstructural development

During grain growth, changes in grain size distribution and in grain shape occurred. The latter was described as spherical particles giving way to nonregular polyhedrons and eventually to mixtures of nearly regular and nonregular polyhedrons. This development was accompanied by removal of the second phase in the set $\{S_P\}$. Both changes are expected to influence properties as a consequence of the relations between macroscopic behaviour and microstructural development; a sensitive property in this regard is the thermal conductivity of the material. The development of the fractal dimension evaluated by this procedure changes during tempering from a value of about 1·15 to a value of 1·10,

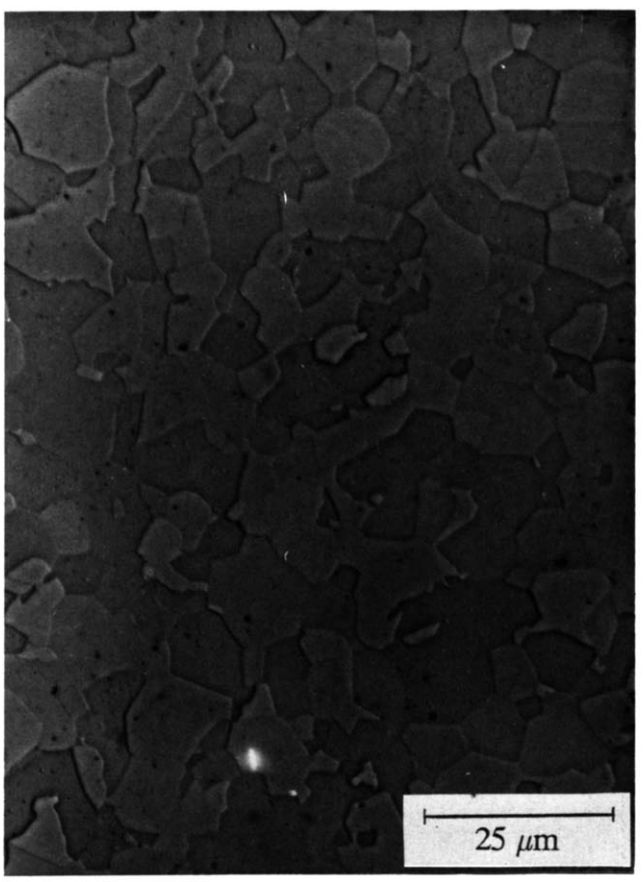

Fig. 4. Optical micrograph of a sample from the set $\{S_P\}$ after 26 h annealing.

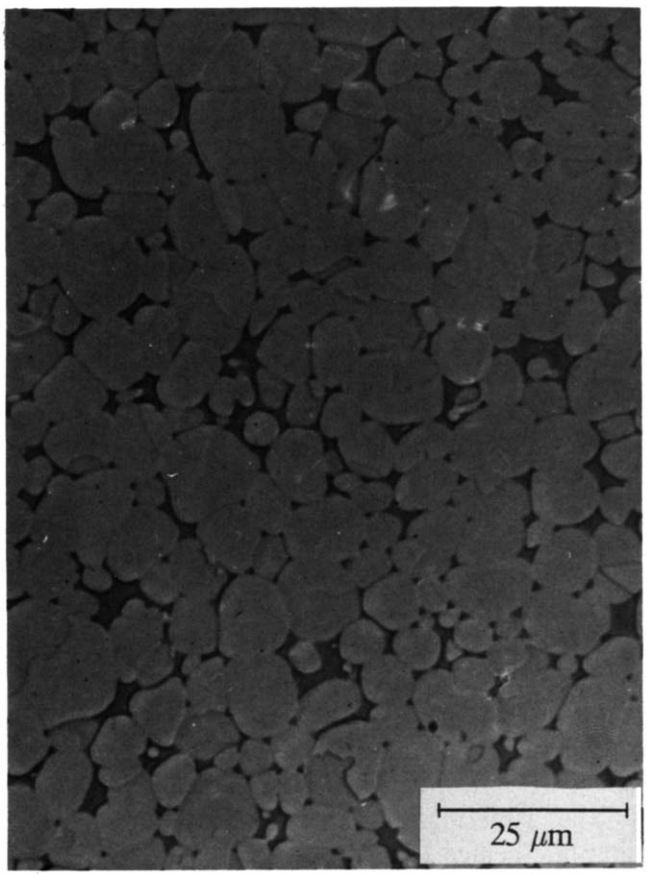

Fig. 5. Optical micrograph of a sample from the set $\{S\}$ after 23·5 h annealing.

indicating loss of curvature during tempering (Fig. 6).

On condition that the chemical composition of the grain boundary phase is constant, it was observed that, over a wide range of tempering time, the thermal conductivity depends approximately linearly on the planarity parameter for both sets of samples (Fig. 7). The reason for this is the bad wetting of the grain boundaries by the $CaO–Al_2O_3$ melt. The marked sample belongs to set $\{S\}$ and exhibits a high content of Ba, 0·4 mass%. The source of this impurity was identified to be the furnace

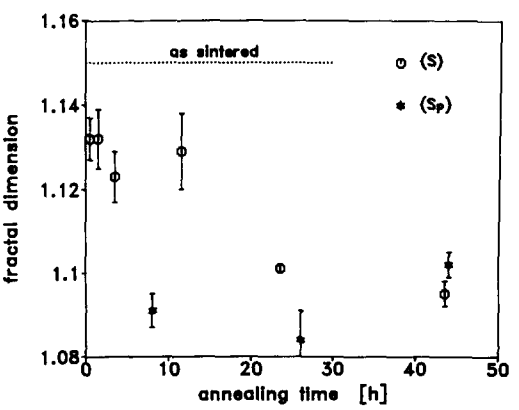

Fig. 6. Fractal dimension of the microstructure of AlN substrate material versus annealing time at a temperature of 1820°C.

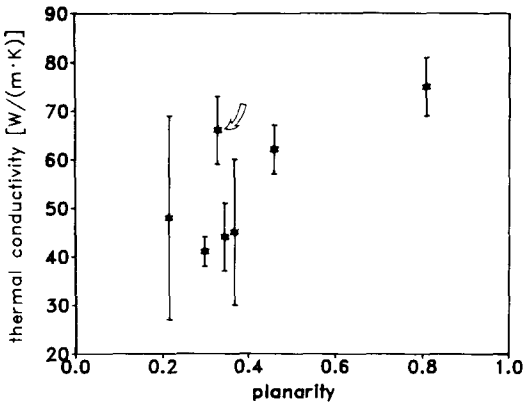

Fig. 7. Thermal conductivity versus planarity parameter.

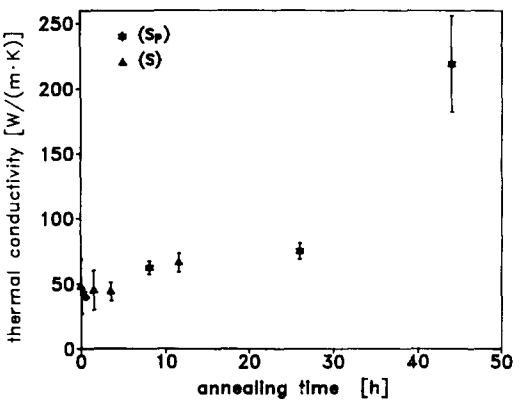

Fig. 8. Thermal conductivity versus annealing time.

atmosphere contaminated by other samples tempered before. Ba is able to trap impurities from the AlN grain, but more rounded AlN grains are formed. Impurity trapping and grain rounding result in contrary effects on the thermal conductivity. This demonstrates once more that impurity trapping is the most effective way to improve the thermal conductivity of AlN ceramics.

With the planarity parameter as defined above, the thermal conductivity is only describable as long as the impurity levels of the grains themselves and the wetting behaviour of the grain boundary phase are similar. As the main impurity in AlN most discussion has related to O, but in the case of this investigation additional Si is detected by EDX analysis on TEM samples. Ca is only detected in the grain boundaries and at line defects, but Si is detected within the grains at a level higher than 1 mass% in relation to the Al content.

The 44-h annealed material from set $\{S_P\}$ exhibits a very high thermal conductivity of (219 ± 37) W $m^{-1} K^{-1}$ (Fig. 8). Within this material, no Si was detectable and Ca and O were only found on a minimum level.

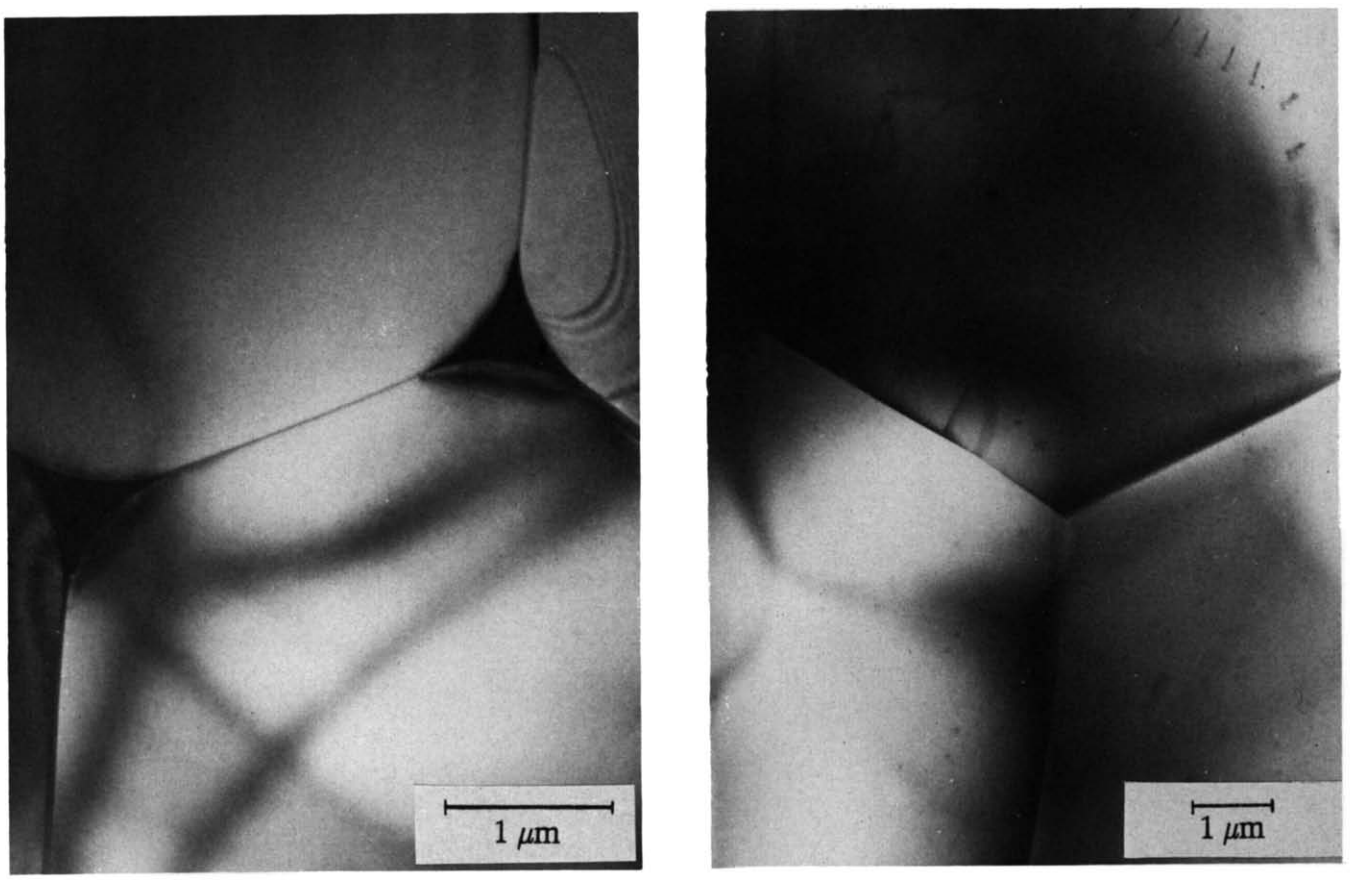

(a) (b)

Fig. 9. (a) TEM micrograph of a 23·5 h annealing sample. (b) TEM micrograph of a material heated for 44 h from set $\{S_P\}$. A chain of parallel dislocation lines is observable in one grain.

If the chemistry of the grains changes, a pure geometric description is not a valid model for the thermal conductivity, because the scattering of phonons by impurities and especially by O and Si in the AlN grains is a strong limiting factor for thermal conduction.[3,9,10]

3.4 TEM observations

Investigations of the microstructure by TEM were done to observe impurities within the grains, and also to detect any defect formation. Even in the very pure materials, lattice dislocation loops were observed (Fig. 9). The grains of the material heated for 23·5 h from sets $\{S\}$ and $\{S_P\}$ were highly disturbed by defects such as dislocations and antiphase boundaries (Fig. 10). In AlN, such line defects can reach very high densities and networks of dislocations have already been observed.[11] Line defects influence the thermal conductivity in proportion to their density and to the absolute value of the Burgers vector (expected to be $\langle 11\bar{2}0\rangle \cdot (a/3)$[11]).

The observed line defects are always connected with precipitates which have been found to include no Al or Si but only Ca. It seems that Ca dissolves in AlN at high temperatures and that precipitates form during cooling if the atoms cannot reach the grain boundary. The mechanical stress produced by the precipitates is a possible source for this building of line defects. Antiphase boundaries are observable even in transparent samples under optical microscopy. Such defects have not been observed by investigators who have used other raw powders and shorter annealing times but the same additive system.[12] During this work the formation of defects is only observed in samples heated for 10 h or more. In other authors' work Y_2O_3-doped samples have exhibited dislocation lines after just 1 h sintering.[11]

4 Conclusions

An increase in the thermal conductivity of AlN up to 219 $W\,m^{-1}\,K^{-1}$ is possible when samples are annealed to evaporate the grain boundary phase. If the chemistry of the AlN grains does not change, a geometrical description of the variation of the grain morphology via topological and fractal arguments is possible to describe the change in thermal conductivity. Impurities are, however, the main source for the phonon scattering and give the main effect on changes in thermal conductivity. In principle, high thermal conductivities can be reached using relatively impure powders but a long isothermal heating is necessary.

The formation of line defects can be influenced either by the sinter additive or by the annealing temperature and annealing time or more probably by all three parameters in some combination.

References

1. Ichinose, N., Aluminum nitride ceramics for substrates. In *Ceramic Developments*, ed. C. C. Sorrell & B. Ben-Nissan. Trans. Tech. Publications Ltd, Switzerland, 1988.

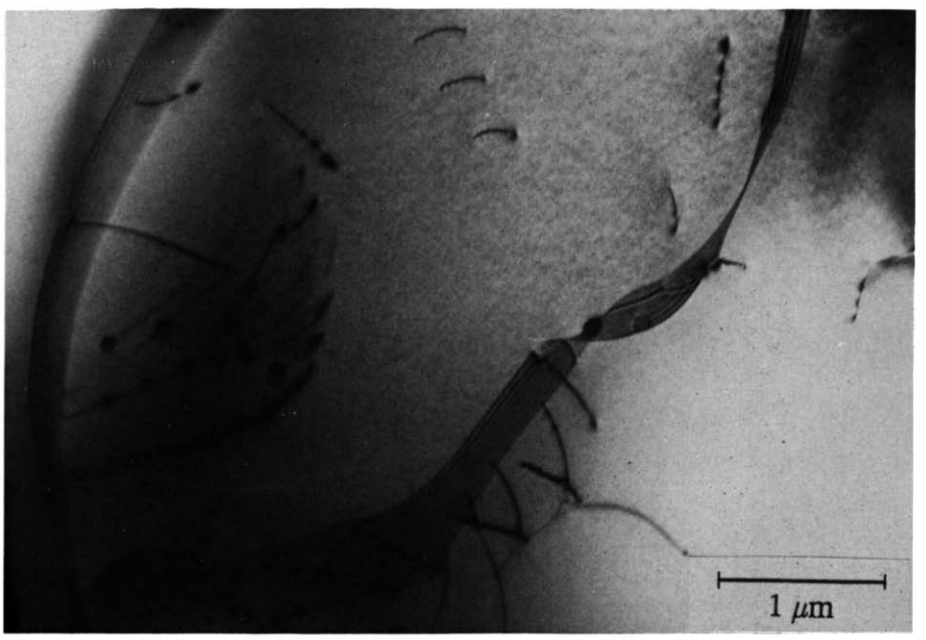

Fig. 10. TEM micrograph of a grain where Ca-containing precipitates associated with dislocations and antiphase boundaries are visible. The material was annealed for 23·5 h and belongs to set $\{S\}$.

2. Shinozaki, K., Iwase, N. & Tsuge, A., High thermal conductive aluminum nitride (AlN) substrates. FC Annual Report (1986) 16.
3. Kranzmann, A., Wärmeleitfähigkeit von drucklos gesinterten AlN-Substratkeramiken. Dissertation, Stuttgart University, FRG, 1988.
4. Niesel, W., Die Dielektrizitätskonstanten heterogener Mischkörper aus isotropen und anisotropen Substanzen, *Annalen der Physik*, **6** (1952) 336.
5. Ondracek, G., Report KfK-2688, Kernforschungszentrum Karlsruhe, Karlsruhe, 1978.
6. Richardson, L. F., General Systems Yearbook, **6** (1961) 139.
7. Mandelbrot, B. B., *The Fractal Geometry of Nature*. W. H. Freeman & Co., New York, 1977, Chapters 3, 12 and 41.
8. Gurland, J., The measurement of grain contiguity in two-phase alloys. *Trans. AIME*, **212** (1958) 452.
9. Kranzmann, A. & Petzow, G., Influence of sinter additives on the thermal conductivity of pressureless sintered aluminum nitride. In *Proceedings of the FEMS*, 1991, in press.
10. Slack, G. A., Tanzili, R. A., Pohl, R. O. & Vandersande, J. W., The intrinsic thermal conductivity of AlN. *J. Phys. Chem. Solids*, **48** (1987) 641.
11. Denanot, M. F. & Rabier, J., Extended defects in sintered AlN. *J. of Mat. Sci.*, **24** (1989) 1594.
12. Kuramoto, N., Taniguchi, H. & Aso, I., Development of translucent aluminum nitride ceramics. *Ceramic Bulletin*, **68** (1989) 883.